A Deep Reinforced Tree-traversal Agent for Coronary Artery Centerline Extraction

Zhuowei Li, Qing Xia(✉), Zhiqiang Hu, Wenji Wang, Lijian Xu, and Shaoting Zhang

SenseTime Research, Beijing, China
{lizhuowei, xiaqing, huzhiqiang, wangwenji, xulijian, zhangshaoting}@sensetime.com

Abstract. Vessel centerline extraction is fundamental for plentiful medical applications. Majority of current methods require pre-segmentations, distance maps or similar sorts of scanning whole volume action and followed by minimal-path or skeletonization algorithms. In this paper, we demonstrate a deep reinforced tree-traversal agent that automatically traces tree-structure centerlines assuming no post-prune or post-merging. It takes raw images as input and generates tree-structure centerlines naturally. To this end, road mark and dynamic reward mechanisms are proposed to make tree-structure vessels learnable and impart the agent how to learn correspondingly. Besides, a multi-task discriminator is raised to simultaneously detect bifurcations and decide terminations. We experimentally show that traced centerlines have an overlap of more than 90% and a distance less than 0.25mm with annotated reference centerlines on coronary arteries. Beyond the promising accuracy, the proposed method also surpasses other existing methods by a large margin in terms of the time and memory efficiency. And a flexible trade-off between accuracy and time efficiency is exhibited at the inference. Codes are available at https://github.com/LzVv123456/Deep-Reinforced-Tree-Traversal

Keywords: Coronary Artery · Centerline Extraction · Reinforcement Learning · Deep Learning

1 Introduction

Vessel centerline extraction is fundamental for plentiful medical applications. It provides, beyond what segmentation and detection provide as *what* and *where*, a more semantic representation of topology and geometry. And as a result, it can facilitate clinical diagnosis and treatment planning.

The vessel centerline extraction problem has been studied for decades. This line of research falls into two general categories: Two-stage methodologies and tracing-based techniques. Majority of current approaches require segmentations, distance maps or similar sorts of scanning whole volume action and followed by minimal-path or skeletonization algorithms [17,5,7,10,11,23,4,6,16,20,14,3,6]. On the contrary, tracing based methods explore local features sequentially [1,4,24,2,8,18,22].

In spite of speed, memory and data efficiency of tracing-based methods, previous tracing methods lack the generalization ability and facing difficulties in handling intricate tree structures. Most recently, Zhang et al. [22] proposed a deep reinforcement learning (DRL) pipeline for aorta centerline tracing. Despite the heuristic functionality of the work, it only deals with single-tubular structures with few orientational variances. Wolterink et al. [18] and Yang et al [21]. on the other hand, train a local navigator with supervised learning. However, it still needs pre-disposed seed points for tree-structure extraction and suffers fussy centerline post-prune and post-merging.

Inspired by the sequential nature of both DRL and tree-traversal process, we here present a **D**eep **R**einforced **T**ree-traversal (DRT) agent that infers tree-structure centerlines from a given initial point. This framework takes raw local patches and generates tree-structured centerlines sequentially. In order to achieve this functionality, three main challenges are addressed as listed:

- *Where is the bifurcation, and when the vessel terminate?* We propose a regression-based **multi-task discriminator** to detect bifurcations and terminations simultaneously. The discriminator essentially models distances between the point of interest and its nearest bifurcation and reference point.
- *In what order should the agent tracing at bifurcations?* We leverage the agent to decide for itself. However, during the training. phase, we propose the **dynamic reward** mechanism to best support and supervise the agent's choice. Specifically, we observe the agent for several steps once meeting a bifurcation, and then we match the path that the agent walks against all the candidate branches. Finally, the best-matched branch wins for the subsequent reward supervision.
- *How to ensure the agent backtrack different branches?* This problem is critical to keep the agent away from trapping in the endless loop. To this end, we come up the **road mark** mechanism to remind the agent of trajectories already passed and serving as a navigation map implicitly.

To evaluate the proposed framework, a dataset contains 280 cardiac CTA images from multiple clinical institutes is collected. Masks of coronary arteries are annotated by experts and centerlines are calculated according to masks followed by manual refinements. In general, our framework surpasses three reproduced baselines (detailed in experiments) by achieving more than 90% overlap rate with less than $0.25mm$ average distances referencing ground-truth centerlines. Beyond the promising accuracy, our framework also outperforms all baselines by a large margin in terms of time and memory efficiency. Extensive ablation studies are further conducted to substantiate proposed innovations.

2 Methods

The centerline tracing process can be viewed as a sequential decision-making process that satisfies the finite Markov Decision Process (MDP) and thus can

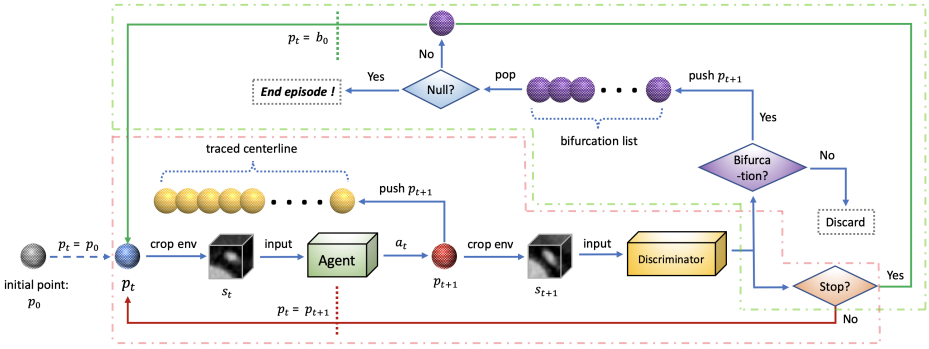

Fig. 1: The general workflow for tree-structured centerline traversal. The red dashed block contains sequential tracing process within a branch and the green dashed block illustrates backtrack routine among separate branches.

be fitted into a standard RL pattern. Then the best policy $q_*(s, a)$ can be approximated by training parameterized network $q(s, a, \theta)$ to minimize:

$$\mathcal{L} = (r_{t+1} + \gamma \max_{a'} q(s_{t+1}, a', \theta^-) - q(s_t, a, \theta))^2 \tag{1}$$

where θ and θ^- parameterize *target network* and *policy network* correspondingly [12]. In our case, *state* s is a 3D local patch cropped at a given point p, *action* a is sampled from the action space A which is N orientations uniformly distributed on a sphere. At each time step, the agent move from current point p_t to p_{t+1} according to action a_t with pre-defined step-size. Once the current trajectory finished, collected points $\{p_0, p_1, ..., p_t\}$ will be deemed as the centerline. In the view of tree structures, we perform tree traversal process as illustrated in Fig. 1. The general process is analog to a depth-first traversal. Despite this intuitive formation, multiple obstacles need to be addressed, and we will plumb these challenges in the following parts of this section.

Reward Design. The goal, *trace centerline*, here can be further decomposed into two sub-goals: (1) trace along the correct direction; (2) trace as close as possible along reference centerlines; Here we propose a target that merges two subgoals into one by directly pulling current proposed centerline point p_t to next target reference point g_{t+k}. Fig. 2 provides a straight forward view of how reward mechanism works (k in Fig. 2 is set to 1 for the sake of interpretation). Given a current proposed point p_t, a corresponding reference point g_t is paired by finding closest point in Euclidean space from the reference centerline. Then the target reference point g_{t+k} is selected from reference centerline sequence with index $t + k$. Then a scalar *trend* T defined as:

$$T = \|v_1\|_2 - \|v_2\|_2 \tag{2}$$

is used to evaluate the pulling action. If $T > 0$, then p_{t+1} is getting closer to g_{t+k} comparing with p_t. Otherwise, it's being pushed away. This scalar T implicitly

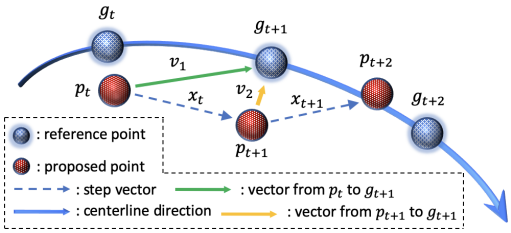

Fig. 2: A straight forward view of reward design. The goal of reward is to encourage the pulling action that pulls current point p_t to objective reference point g_{t+1}.

convey the goodness of the sampled orientation. Depending on the *trend*, the *reward* is designed as:

$$R = \begin{cases} \frac{T}{2\|x_t\|_2} + A & \text{if } T > 0. \\ 0 & \text{otherwise.} \end{cases} \tag{3}$$

A is an auxiliary signal employed to encourage proposed point to stay around the reference centerline. Explicit expression for A is: $A = \frac{1}{1+e^{-x}}$ where x is point to curve distance defined as L_2 distance from p_{t+1} to it's nearest reference point.

Road Mark. Considering the single vessel situation where only a single tubular structure exists. The main challenge emerges as ambiguous orientation information. The vessel centerline can be viewed as a directed curve from the proximal point to the distal point. Under a tracing framework, global information is commonly not available, and the local patch can have a similar appearance towards both proximal and distal directions. This will cause conflicts during training and potentially cause 'look back' or even 'stay around' during inference. Regarding tree structures at the inference process, the agent will trace the identical branch due to its deterministic essence unless manual interventions are imposed. Here, we propose a simple yet effective solution, namely ***road mark***, for both scenarios. As indicated by the name and showed in Fig. 3, a distinctive mark (a cube with size n and value c in our setting) is left to the raw environment where the agent has passed. By doing so, we transfer the directional and ordinal information into visual features that can be directly encoded into the neural network. The road mark prevents the agent from hesitation as well as indicating tracing order at bifurcations.

Dynamic Reward. With the assistance of the road mark, the topological information can be reconstructed by purely learning local patches. Nevertheless, it is still an open question on how to learn at bifurcations. Specifically, in what order should the agent trace at bifurcations. We speculate that any hand-crafted rules can lead to sub-optimum. Based on this conjecture, we propose the ***dynamic reward*** mechanism to leverage the agent itself to decide the tracing order during training. A buffer zone equaling to Z time steps is created when

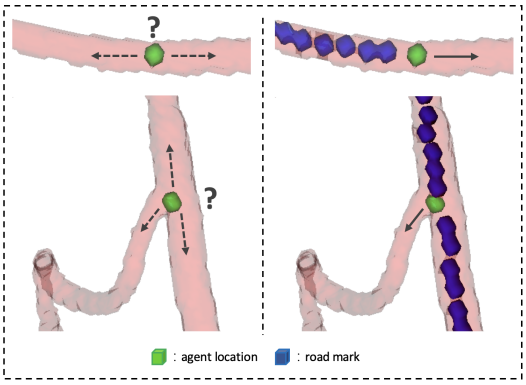

Fig. 3: Left side and right side of the figure displays a real environment with and without the road mark correspondingly. Road marks in the vessel served as the orientation indicator.

reaching a bifurcation. Then accumulated rewards $R_n = \sum_{i=1}^{Z} r_i$ within Z continuous time steps according to all N potential candidates are collected. And the candidate with index equal to $argmax(R_0, R_1, ..., R_{N-1})$ is set as the reference centerline. Once a reference centerline is decided, other candidates will be ignored and get back to single vessel mode. Within the buffer zone range, the agent is always awarded the largest reward regardless of which candidates it relies on. When the agent backtracks to the same bifurcation, the reference centerline already used will be disregarded from the candidate pool, then the same strategy is executed again. This mechanism provides a dynamic control over rewards and reference centerline at bifurcation during the training.

Multi-task Discriminator. Herein, a ***multi-task discriminator*** is trained separately to regress distances from a point to it's nearest bifurcation and reference point simultaneously. The training data is generated by random sampling points from reference centerlines with jittering (a 3D Gaussian distribution parameterized by $\mu = 0, \sigma = 10$ is used for jittering). Two ground truth scalars for each training point are decided using an identical formula:

$$G = \begin{cases} e^{a(1-\frac{D(x)}{d_M})} - 1 & \text{if } D(x) < d_M. \\ 0 & \text{otherwise.} \end{cases} \tag{4}$$

proposed by Sironi et al. [15]. $D(x)$ is the $\mathcal{L}_2$ distance between the sampled point x and it's target point. a is set to 6 as explored in the original paper and d_M is set to half of the patch size. Then a weighed MSE loss defined as: $\mathcal{L} = \frac{\mathcal{L}_1}{2} + \frac{\mathcal{L}_2}{2}$ is minimized. During the inference, the discriminator slides together with the agent along the vessel and a window of passed proximity values are maintained. Then the local maximums are extracted immediately as bifurcations and the termination will be triggered if the average value of the corresponding proximity

map exceeds certain threshold $\mathcal{T}$ which means the current location is no longer close to any reasonable reference centerline.

Train and Inference. The tracing agent is trained episodically. Within an episode, the 3D volumetric image and centerlines formed as directed graphs are collected. The agent is initialized around the root of the tree structure and training by conducting tracing. Once the agent successfully reaches a bifurcation, it will act according to the dynamic reward mechanism and activate this bifurcation. The current trajectory terminates if one of the following criteria satisfied: (1) reach a distal point; (2) go out of the safe range; (3) reach predefined maximum steps; Once a trajectory is ended, the agent will backtrack from an activated bifurcation and deactivate this bifurcation once there is no trainable candidate branch. The whole episode ends until there is no existing activated bifurcation. During inference, given a root point, the agent has already equipped with the knowledge on how to trace and in what order to trace. Noticing that the discriminator is trained independently and no road mark mechanism is applied for the discriminator. So we also maintain a clear environment for the discriminator during inference.

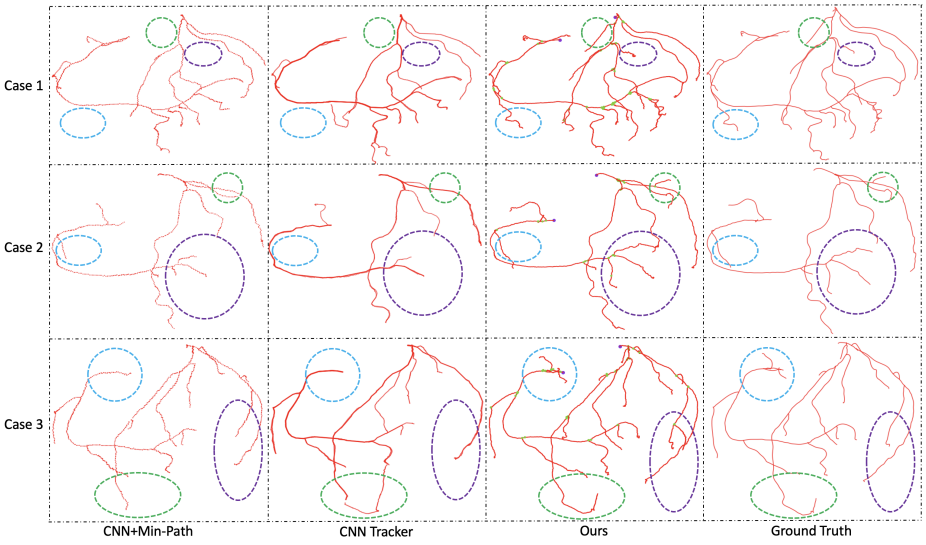

Fig. 4: Centerlines are displayed using scatters and all results remain their original appearance without post-processing. Tiny green points in our methods are bifurcations detected and two larger purple points are ostium location. According to this visualization result, our method achieved better completeness and acting less prone to over-tracing.

3 Experiments and Results

Dataset. We collect a cardiac CTA dataset that contains 280 patients from 4 clinical institutions. Most of these patients contain a certain degree of stenosis and plaques. And masks of all feasible coronary arteries are deliberately annotated by experts, and centerlines are extracted using TEASAR [13]. Furthermore, centerlines extracted are scrutinized and manually refined. All centerlines are formed as directed acyclic graph (DAG) for the final input. In experiments, images are resampled isotropically to spacing 0.5mm, and intensities are normalized between 0 and 1. The whole dataset is randomly split into 140 training and 140 validation.

	overlap (%)			distance (mm)			time cost (s)		
Method	max	min	average	max	min	average	max	min	average
MSCAR-DBT+skeletonization	96.41	47.68	81.66	0.4193	0.2865	0.3437	26.32	14.01	20.12
CNN+Min-Path	97.46	**74.78**	89.29	**0.3102**	0.2055	0.2608	**25.50**	18.84	21.93
CNN Tracker	98.79	42.78	89.18	0.357	0.2266	0.2929	59.9	7.89	28.40
Ours	**100.00**	54.93	**90.05**	0.3478	**0.1966**	**0.2491**	30.48	**4.32**	**13.11**

Table 1: Comparison of proposed method against three baselines with respect to metrics of both accuracy and efficiency. Our method surpasses three baselines in terms of both accuracy and efficiency.

Metric. We evaluate the result of each patient in two aspects: ***overlap*** (a combination of point-level precision and recall) and ***distance***, similar to what is used in Zhang et al. [22]. Given two sets of 3D points, one for reference centerline and another for traced centerline (Both centerlines are resampled to 0.025mm for an accurate calculation). The corresponding point for a given point is defined as the nearest point on the opposite set. A point is covered if Euclidean distance between it and its corresponding point is less than threshold H_m (we set $H_m = 1$mm across all experiments) and missed otherwise.

Formally, if a reference point is covered, we marked it as R_t and R_f otherwise. Similarly, a traced point will be marked as T_t or T_f regarding the case. With $||.||$ denoting the cardinality of the set of points, the overlap is defined as:

$$\alpha \frac{\|T_t\|}{\|T_t\| + \|T_f\|} + (1-\alpha) \frac{\|R_t\|}{\|R_t\| + \|R_f\|} \tag{5}$$

As for distance, D_r is defined as average Euclidean distance between matched points in reference and their corresponding traced points. And D_t is defined analogously with reversed direction. Then the distance is defined as: $\alpha D_r + (1-\alpha)D_t$. α is set to 0.5 for both metrics.

Coronary Artery Centerline Extraction. Herein, three methods range from pure traditional methods to solo deep learning methods are reproduced as baselines. We first reproduced SOTA tracing method ***CNN Tracker*** [18].

Since we do not assume the acquisition of vessel radius, all radius-related parameters are set to 1mm. Other parameters remained the same as the original work. The second baseline is a combination of CNN segmentation with minimal path extraction (***CNN+Min-Path***). Two segmentation models from coarse to fine are trained according to Xia et al. [19] with our annotated coronary artery masks. Then centerlines are extracted from a fine-grained segmentation mask using a TEASAR [13] algorithm. At last, we also reproduced a traditional centerline extraction method (***MSCAR-DBT+skeletonization***), coronary artery masks are extracted according to MSCAR-DBT [24] and centerlines are acquired through skeletonization operation [9]. The architecture used in our work is the same as what was proposed in the CNN Tracker to perform an impartial comparison. Ostium locations are provided for both CNN Tracker and our method for the sake of justice. As displayed in Table 1, Our methods surpass all baselines in terms of both accuracy and efficiency. CNN Tracker failed to track several sub-branches, and it is prone to over-tracing. CNN+Min-Path suffers from segmentation errors and shortcuts caused by the minimal path. And traditional method falls behind in general due to its weak generalization ability. Fig. 4 visualizes three cases. Step-size at inference can be set arbitrarily within a reasonable range regardless of training step-size. Here we measure step-size from 0.5 to 2.0. As shown in Table 2, there is a trade-off between speed and quality. According to experiments, step-size equaling to 1.0 generates the highest cost performance. It only takes around 5 seconds for each patient with little damage in accuracy.

step-size	average overlap (%)	average distance (mm)	average time cost (s)
0.5	90.05	0.2491	13.11
0.6	89.64	0.2511	10.52
0.7	89.44	0.2549	9.76
0.8	89.58	0.2574	7.11
0.9	89.19	0.2638	6.06
1.0	89.36	0.2673	5.68
1.1	89.38	0.2758	5.57
1.2	89.39	0.2830	5.16
1.3	88.49	0.2884	4.55
1.4	87.63	0.2947	4.16
1.5	88.03	0.3021	4.05
1.6	86.31	0.3092	3.57
1.7	86.57	0.3175	3.39
1.8	85.82	0.3246	3.01
1.9	84.48	0.3328	2.72
2.0	83.54	0.3433	2.49

Table 2: Detail results for different step-size.

Variations	average overlap (%)	average distance (mm)
no-mark+random	60.59	0.3443
no-mark+order	62.67	0.3135
no-mark+angle	63.54	0.3102
no-mark+dynamic	61.07	0.3029
mark+random	76.41	0.3160
mark+order	89.05	0.2632
mark+angle	92.86	0.2482
mark+dynamic	**93.74**	**0.2447**

Table 3: Road mark combined with dynamic reward outperform all other combinations.

Ablation Studies. We demonstrate the effectiveness of the road mark and dynamic reward mechanism in this section. Ground truth bifurcations and termi-

nations are provided across ablation studies to avoid perturbation caused by the discriminator. 8 variations are implemented to interpret road mark and dynamic reward, ***mark*** and ***no-mark*** represents whether utilize road mark or not. Four different training modes at bifurcations are disposed: (1) randomly select a sub-branch at bifurcations (***random***); (2) always choose the sub-branch with least accumulated x coordinate values (***order***); (3) always choose the sub-branch with the least angle referencing it's father-branch (***angle***); (4) our dynamic reward mode (***dynamic***). As showed in Table 3, road mark enabled tree structure tracing. According to our off-line visualization results, the agent will always trace the same path and sometimes traces loops without a road mark. Dynamic reward surpassed all three other manually designed training modes. The most allied results came from the angle mode, which also satisfies the common intuition.

4 Conclusion and Future Work

This work presents a novel framework for tree-structure vessel centerline tracing and demonstrates promising results on coronary artery centerline extraction. Unlike other existing learning-based methods. This framework is designed and boosted to consume DAG and infer the tree-structure naturally. However, due to the sequential tracing nature, its advantage in efficiency will degrade confronting non-sparse environments. For future improvement, it will be more elegant and efficient to further merge the agent with the discriminator.

Acknowledgements This work was supported by the Beijing Postdoctoral Research Foundation, the Beijing Nova Program (Z201100006820064), the Shanghai Xuhui District HealthCare AI Cooperation Project (2020-011) and the National Key Research and Development Project of China (2020YFC2004800).

References

1. Aylward, S.R., Bullitt, E.: Initialization, noise, singularities, and scale in height ridge traversal for tubular object centerline extraction. IEEE Transactions on Medical Imaging **21**(2), 61–75 (Feb 2002)
2. Cetin, S., Unal, G.: A higher-order tensor vessel tractography for segmentation of vascular structures. IEEE Transactions on Medical Imaging **34**(10), 2172–2185 (Oct 2015)
3. Cui, H., Xia, Y.: Automatic coronary centerline extraction using gradient vector flow field and fast marching method from ct images. IEEE Access **6**, 41816–41826 (2018)
4. Friman, O., Kuehnel, C., Peitgen, H.: Coronary centerline extraction using multiple hypothesis tracking and minimal paths (07 2008)
5. Gülsün, M.A., Funka-Lea, G., Sharma, P., Rapaka, S., Zheng, Y.: Coronary centerline extraction via optimal flow paths and cnn path pruning. In: Medical Image Computing and Computer-Assisted Intervention – MICCAI 2016. pp. 317–325. Springer International Publishing, Cham (2016)

6. Guo, Z., Bai, J., Lu, Y., Wang, X., Cao, K., Song, Q., Sonka, M., Yin, Y.: Deepcenterline: A multi-task fully convolutional network for centerline extraction. ArXiv **abs/1903.10481** (2019)
7. Jin, D., Iyer, K.S., Chen, C., Hoffman, E.A., Saha, P.K.: A robust and efficient curve skeletonization algorithm for tree-like objects using minimum cost paths. Pattern Recogn. Lett. **76**(C), 32–40 (Jun 2016)
8. Lesage, D., Angelini, E.D., Funka-Lea, G., Bloch, I.: Adaptive particle filtering for coronary artery segmentation from 3d ct angiograms. Computer Vision and Image Understanding **151**, 29 – 46 (2016), probabilistic Models for Biomedical Image Analysis
9. Maragos, P.A., Ronald, Schafer, W.: Morphological skeleton representation and coding of binary images. IEEE Trans. Acoustics, Speech and Signal Processing (1986)
10. Metz, C.T., Schaap, M., Weustink, A.C., Mollet, N.R., van Walsum, T., Niessen, W.J.: Coronary centerline extraction from ct coronary angiography images using a minimum cost path approach. Medical Physics **36**(12), 5568–5579 (2009)
11. Mirikharaji, Z., Zhao, M., Hamarneh, G.: Globally-optimal anatomical tree extraction from 3d medical images using pictorial structures and minimal paths. In: Medical Image Computing and Computer-Assisted Intervention MICCAI 2017. pp. 242–250. Springer International Publishing, Cham (2017)
12. Mnih, V., Kavukcuoglu, K., Silver, D., Graves, A., Antonoglou, I., Wierstra, D., Riedmiller, M.: Playing atari with deep reinforcement learning. arXiv preprint arXiv:1312.5602 (2013), https://arxiv.org/pdf/1312.5602.pdf
13. Sato, M., Bitter, I., Bender, M.A., Kaufman, A.E., Nakajima, M.: Teasar: tree-structure extraction algorithm for accurate and robust skeletons. In: Proceedings the Eighth Pacific Conference on Computer Graphics and Applications. pp. 281–449 (Oct 2000). https://doi.org/10.1109/PCCGA.2000.883951
14. Schaap, M., van Walsum, T., Neefjes, L., Metz, C., Capuano, E., de Bruijne, M., Niessen, W.: Robust shape regression for supervised vessel segmentation and its application to coronary segmentation in cta. IEEE Transactions on Medical Imaging **30**(11), 1974–1986 (Nov 2011)
15. Sironi, A., Lepetit, V., Fua, P.: Multiscale centerline detection by learning a scale-space distance transform. In: 2014 IEEE Conference on Computer Vision and Pattern Recognition. pp. 2697–2704 (June 2014)
16. Stefancik, R., Sonka, M.: Highly automated segmentation of arterial and venous trees from three-dimensional magnetic resonance angiography (mra). The international journal of cardiovascular imaging **17**, 37–47 (03 2001)
17. Wink, O., Frangi, A.F., Verdonck, B., Viergever, M.A., Niessen, W.J.: 3d mra coronary axis determination using a minimum cost path approach. Magnetic Resonance in Medicine **47**(6), 1169–1175 (2002)
18. Wolterink, J.M., van Hamersvelt, R.W., Viergever, M.A., Leiner, T., Išgum, I.: Coronary artery centerline extraction in cardiac ct angiography using a cnn-based orientation classifier. Medical Image Analysis **51**, 46 – 60 (2019)
19. Xia, Q., Yao, Y., Hu, Z., Hao, A.: Automatic 3d atrial segmentation from ge-mris using volumetric fully convolutional networks. In: Pop, M., Sermesant, M., Zhao, J., Li, S., McLeod, K., Young, A., Rhode, K., Mansi, T. (eds.) Statistical Atlases and Computational Models of the Heart. Atrial Segmentation and LV Quantification Challenges. pp. 211–220. Springer International Publishing, Cham (2019)
20. Yang, G., Kitslaar, P., Frenay, M., Broersen, A., Boogers, M.J., Bax, J.J., Reiber, J.H.C., Dijkstra, J.: Automatic centerline extraction of coronary arteries in coro-

nary computed tomographic angiography. The International Journal of Cardiovascular Imaging **28**(4), 921–933 (Apr 2012)
21. Yang, H., Chen, J., Chi, Y., Xie, X., Hua, X.: Discriminative coronary artery tracking via 3d CNN in cardiac CT angiography. In: Shen, D., Liu, T., Peters, T.M., Staib, L.H., Essert, C., Zhou, S., Yap, P., Khan, A.R. (eds.) Medical Image Computing and Computer Assisted Intervention - MICCAI 2019 - 22nd International Conference, Shenzhen, China, October 13-17, 2019, Proceedings, Part II. Lecture Notes in Computer Science, vol. 11765, pp. 468–476. Springer (2019)
22. Zhang, P., Wang, F., Zheng, Y.: Deep reinforcement learning for vessel centerline tracing in multi-modality 3d volumes. In: Frangi, A.F., Schnabel, J.A., Davatzikos, C., Alberola-López, C., Fichtinger, G. (eds.) Medical Image Computing and Computer Assisted Intervention – MICCAI 2018. pp. 755–763. Springer International Publishing, Cham (2018)
23. Zheng, Y., Tek, H., Funka-Lea, G.: Robust and accurate coronary artery centerline extraction in cta by combining model-driven and data-driven approaches. In: Medical Image Computing and Computer-Assisted Intervention – MICCAI 2013. pp. 74–81. Springer Berlin Heidelberg, Berlin, Heidelberg (2013)
24. Zhou, C., Chan, H.P., Chughtai, A., Patel, S., Hadjiiski, L.M., Wei, J., Kazerooni, E.A.: Automated coronary artery tree extraction in coronary ct angiography using a multiscale enhancement and dynamic balloon tracking (mscar-dbt) method. Computerized Medical Imaging and Graphics **36**(1), 1 – 10 (2012)